To cite this document:
H. Zia, B. Lecampion, Explicit versus implicit front advancing schemes for the simulation of hydraulic fracture growth, *Int. J. Numer. Anal. Meth. Geomechanics*, (2019) https://doi.org/10.1002/nag.2898

Submitted on 20 July 2018, revised 31 October 2018, accepted 6 December 2018.

Explicit versus implicit front advancing schemes for the simulation of hydraulic fracture growth

Haseeb Zia[a], Brice Lecampion[a,*]

[a]*Geo-Energy Lab - Gaznat chair on Geo-Energy,*
Swiss Federal Institute of Technology Lausanne, EPFL, Lausanne, Switzerland

Abstract

The proper computation of the time evolution of the fracture front is the main challenge of 3D hydraulic fracture growth simulation. We discuss explicit and implicit variants of a hydraulic fracture propagation scheme based on a level set representation of the fracture. Such a scheme couples a finite discretization of the governing equations and the near-tip hydraulic fracture asymptotes. We benchmark the accuracy, robustness and stability of these different front advancing schemes on a number of test cases. Our results indicate a large computational gain of the explicit scheme at the expense of a slightly less accurate solution (few percent less accuracy over few time-steps) when crossing heterogeneities. The predictor corrector scheme combines at least a $\sim$ 25% computational gain while retaining the stability and accuracy of the fully implicit version of the scheme in all cases.

Keywords: Hydraulic fracture propagation, Level set method, moving boundary problem, explicit vs. implicit schemes

1. Introduction

Hydraulic fractures are a class of tensile fractures that propagate in a material due to the injection of a viscous fluid [1]. A mathematical model of hydraulic fracture growth needs to account for the elastic deformation of the medium, the creation of new fracture surface as well as the flow of viscous fluid inside the created fracture and its potential leak-off in the surrounding rock [2, 3]. Fracture propagation is intrinsically a moving boundary problem where the time evolution of the

*Corresponding author: Brice.Lecampion@epfl.ch

fracture front is to be determined. The coupling between the elastic deformation of the fracture and the flow of viscous fluid inside is highly non-linear and results in an extremely stiff system. Combined with the fracture propagation condition, such an elasto-hydrodynamics system yields an intricate multiscale structure near the fracture tip where different asymptotes emerge at different lengthscales as function of the rock and fluid properties as well as the current fracture velocity. It has been recognized for some time that the linear fracture mechanics asymptote can shrink to a boundary layer at the fracture tip in the so-called viscosity dominated regime [4, 5, 6, 7]. This renders numerical schemes based solely on the linear elastic fracture mechanics propagation condition rather inefficient in those cases, and poses a significant challenge to any numerical scheme. It is important to point out that the fracture velocity is a-priori unknown and varies temporally as well as spatially around the fracture front.

Peirce and Detournay [8] presented an implicit level set algorithm that does not require the a-priori knowledge of the fracture front velocity to evolve the fracture front over a time-step. The distinguishing feature of this scheme is its use of the hydraulic fracture tip asymptote solution valid close to the fracture tip [9, 10, 7]. Incorporating this near-tip solution in a numerical algorithm based on a finite discretization of the fracture results in a robust and accurate scheme even on a relatively coarse mesh. This allows one to capture the different physical processes occurring at small scales near the tip accurately in a computationally efficient manner. In such a scheme, the fracture velocity is obtained all around the fracture front as part of the solution over a time-step. These advantages make the Implicit Level Set Algorithm (ILSA) a very accurate numerical scheme for any given mesh resolution as can be seen by the benchmarks against known analytical solutions [8, 11, 12, 13].

Since the velocity of the fracture front is not available a-priori, ILSA determines the location of the front "implicitly" via an iterative process. An alternative to this scheme is to advance the front "explicitly": using the velocity of the fracture front estimated from the last time step. This choice may possibly introduce error in the solution, especially if the fracture front passes through heterogeneities (stress, material changes etc.), due to over or under predictions of the velocity depending upon the nature and magnitude of the heterogeneity. It is unclear a-priori how the choice of the time-step may influence the accuracy of such an explicit scheme. The advantage, on the other hand, is that it can reduce the computational cost many folds as each of the fracture front iterations of the implicit scheme cost the equivalent of one explicit step.

In this paper, we compare the performance of the implicit level set algorithm

(ILSA) with an explicit version of the scheme as well as a predictor corrector version that uses the front provided by the explicit step as the first trial position for the implicit scheme. We assess the gain in the computational efficiency of the explicit scheme as well as its potential loss of accuracy and stability on different verification cases. Although we restrict our discussion to the case of planar 3D hydraulic fractures, we believe that similar performance will be shown by the explicit scheme for full 3D problems, where the front is constituted by a surface which can move in any direction in 3D, as well as for bi-dimensional configurations, where the fracture front is reduced to two points and can move only along a line.

It is important to note that the choice of an explicit or implicit scheme for the fracture front advance is distinct from the choice of an implicit or explicit time discretization of the coupled fluid flow/elasticity equations for a given fracture geometry. Due to the stringent CFL condition of the elasto-hydrodynamics system for a given fracture advance [2], the variants of the original ILSA scheme that we present also use an implicit (Backward Euler) scheme to solve the fluid-solid coupling: the explicit nature of the scheme is solely restricted to the fracture front advance over a time-step.

2. Numerical modeling of planar hydraulic fracture growth

We consider here a planar (pure mode I) 3D hydraulic fracture driven by the injection of a viscous fluid into a linear elastic medium under a pre-existing compressive stress field. The plane of propagation ($z = 0$) is oriented perpendicular to the minimum in-situ compressive stress $\sigma_o(x, y)$. We follow the classical assumptions of hydraulic fracture mechanics [1] which rely on coupling linear elastic fracture mechanic, lubrication fluid flow in the fracture and an early-time approximation for fluid leak-off from the fracture into the surrounding medium (Carter's leak-off). For a detailed discussion of such a classical hydraulic fracture model and its formulation, we refer to e.g. [14, 1, 3].

We only present here the necessary information on the numerical discretization of the problem using the implicit level set algorithm (ILSA) developed in [8, 12, 13, 15]. During a time step, ILSA consists of two nested loop. The outer loop iterates on the new fracture front, while the inner loop solves the coupling between elasticity and fluid flow for the corresponding given trial fracture front position and tip behavior.

For a planar 3D hydraulic fracture, the elasticity equations reduce to a single boundary integral equation for opening mode that is solved using piece-wise con-

stant rectangular displacement discontinuity [16]. The fracture front is tracked by a level set and the front is reconstructed in a piece wise linear fashion in the tip elements (see Figure 1). The lubrication flow inside the fracture is discretized using a five-point stencil finite difference with the fluid pressure located at the center of the rectangular displacement discontinuity element. The coupling between elasticity and fluid flow yields - for a given trial fracture front - a non-linear system of equations that we solve via fixed point iterations. It is worth emphasizing that this non-linear system is constructed using a backward Euler scheme for the time derivative entering into the lubrication equation. This choice stems from the very restrictive CFL condition for such an elasto-hydrodynamics system of equations which is given as $\Delta t < h^3/E'D$ [2], where h is the grid size and $D \approx \bar{w}^3/\mu$ is a diffusivity coefficient function of a nominal fracture width $\bar{w}$). One clearly sees that an explicit (forward Euler) scheme for such a coupled system would result in extremely small time-step size and would thus be extremely expensive. It is however important to note that the time stepping scheme for the evolution of the fracture front over a time-step may actually be chosen differently as will be discussed below.

The quasi-static fracture propagation condition all along the fracture front closes the system of equations, i.e. $K_I(x_c) = K_{Ic}$ where K_I is the mode I stress intensity factor and K_{Ic} the material fracture toughness. It can be shown that the fluid and fracture front coalesce when the in-situ stress σ_o is sufficiently large [4], more precisely, for time larger than $E'^2\mu/\sigma_o^3$ [17, 18]. Under those circumstances [14], the additional boundary conditions at the fracture front are of zero fluid flux $q = wV = 0$ (where V is the fluid velocity equals to the fracture tip velocity in the absence of lag) and zero width w. The fracture velocity can not therefore be explicitly recovered. The key idea of the implicit level set scheme is to use the tip asymptotic solution of a steadily moving hydraulic fracture. Indeed, in the vicinity of the fracture front, the planar 3D problem at a given time reduces asymptotically to the one of a semi-infinite plane-strain hydraulic fracture propagating at a constant velocity V. This so-called 'tip problem'has been addressed and solved in details [9, 6, 7]. The fracture width and net pressure have been shown to transition from the classical linear elastic fracture mechanics asymptote near the tip to the viscosity dominated asymptote [9] away from the tip over a length scale governed by the problem parameters [7]. The effect of fluid leak-off appears as an intermediate asymptote [10, 7] between the LEFM and the viscosity dominated asymptote. Such a tip asymptotic solution which embeds the different non-linearities of the problem has been shown to be valid over a large part of the fracture for the fracture width. It can be used in combination with a finite scale

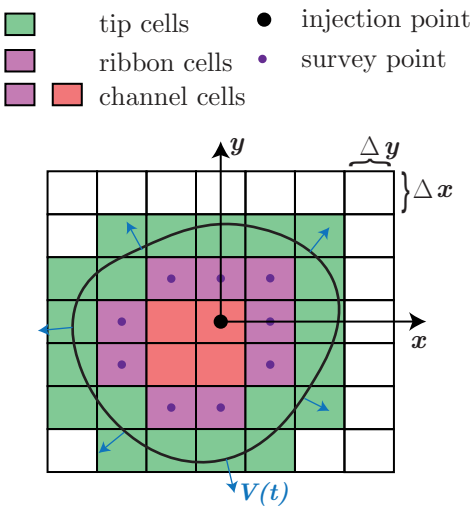

Figure 1: The fracture plane is discretized with a Cartesian mesh using rectangular cells. At any time, the cells are classified as either tip (near the front) or channel cells. Among the channel cells, the cells adjacent to the tip cells are denoted as ribbon cells (with their centers as survey points) and are used to coupled the finite discretization with the near-tip hydraulic asymptotic solution (see e.g.[12] for more details).

discretization in order to obtain very efficient schemes even on a coarse mesh [8, 11]. The tip solution for the fracture width can be schematically written as:

$$\hat{w} = f(s, V, E', K_{Ic}, \mu, C_L), \tag{1}$$

where $\hat{w}$ is the width of the fracture in the tip region and s is the closest distance from fracture front. Conversely, knowing the fracture width, this function can be inverted to get the distance to the fracture front from the survey point where the width is estimated. This allows for construction of efficient and accurate numerical schemes combining this tip solution with a finite discretization and a level set approach to evolve the fracture front over a time-step [8, 12, 13].

3. Fracture front advancing schemes

We now describe the different possible schemes that can be used to advance the fracture front and the solution over a time step, given an initial fracture foot-

print in equilibrium with both the elasto-hydrodynamics equations and the fracture propagation condition. All these schemes are based on a level set representation of the fracture front and the use of the hydraulic fracture tip asymptotic solution Eq. (1).

3.1. Implicit front advance

This is the original (implicit) version of the level set scheme proposed by [8]. We recall it here for clarity and completeness (more details can be found in [8, 12, 13, 15]). The steps taken by the algorithm to advance the fracture over a time step from t^n to $t^{n+1} = t^n + \Delta t$ can be summarized as follows.

Injection with the same footprint:. The implicit algorithm starts with a balloon like inflation of the fracture on the previous fracture footprint at t^n. This is performed by solving the coupled elasto-hydrodynamic system with the previous fracture footprint to evaluate a new fracture width - which is inflated if the injection continue and the fracture footprint does not change.

Inversion of the tip asymptote. From the current footprint of the fracture, the channel cells neighboring tip cells are taken as survey cells (referred as ribbon cells in the rest of the paper; see Figure 1). The width of the ribbon cells from the inflated fracture is then used to invert the tip asymptote to obtain the minimum distance of the center of these ribbon cells to the new fracture front. It is important to note here that the local fracture velocity of the front appears as a variable in the tip asymptote function that provides the relation between the width and the tip distance (Eq. 1). At the stage of tip inversion, the velocity at time t^{n+1} is not readily available and is thus approximated via an implicit (backward-Euler) approximation:

$$V^{n+1} = \frac{s^{n+1} - s^n}{\Delta t}, \tag{2}$$

where Δt is the time step, s is the distance from the front and the superscript $n + 1$ refer to the time t^{n+1}. This makes the tip asymptote an implicit function of the form

$$\hat{w} = f(s^{n+1}, \frac{s^{n+1} - s^n}{\Delta t}, E', K_{Ic}, \mu, C_L), \tag{3}$$

which can be solved via a root finding algorithm for s^{n+1}. We use the efficient approximation of the complete hydraulic fracture tip asymptote presented in Dontsov and Peirce [15].

Reconstruction of the fracture front. The fracture front is represented via a signed distance function on the computational domain (a level set), which is initialized with the given tip distances at the ribbon cells. The distances are initialized as negative to impose the sign convention that these cells are located inside the fracture. Knowing the closest distance to the fracture front at each ribbons cells, the Eikonal equation is then solved in the rest of the grid via the Fast Marching Method. From the knowledge of the signed distance function at every cell of the grid, the fracture front is constructed by identifying the zero level set i.e. the set of points where the signed distance has a value of zero (see [8] for details). Note that the level set provides the front location at sub-mesh scale, i.e. the front is tracked irrespective of the mesh resolution.

Tip volume calculation. After the new fracture front position has been determined, the average fracture width in the tip cells are evaluated by averaging the hydraulic fracture tip asymptote over these cells, thus imposing the proper fracture volume in the tip cells. Projecting the one dimensional tip asymptotic solution on to two dimensions and its integration over the tip cells is discussed at length in [15] which provides efficient computations of these different integrals over the tip cells.

Solution of the elasto-hydrodynamic system. Once a new fracture front position is determined and the tip volumes evaluated, all the terms required to make a new elasto-hydrodynamic system are available. The system is then solved iteratively via fixed point iterations to determine the corresponding new width of the channel cells and pressure of the tip cells.

From this new solution, the width of the ribbon cells are again inverted to get a new footprint. The overall iterative procedure is repeated until the front position converges. The iterations are stopped once the average of the difference in the filling fractions of all the tip cells between two successive iterations is less than 10^{-3}. The overall iterative procedure is summarized in the form of a flow chart in Figure 2.

3.2. Explicit front advance

For each iteration of the implicit front advancing algorithm, the front position is found by inverting the tip asymptote. Due to the direct correspondence between the front position and the propagation velocity (see Eq. (2)), the fracture front iteration can also be viewed as an iteration on the propagation velocity at all points along the fracture front. This iterative process is computationally expensive as

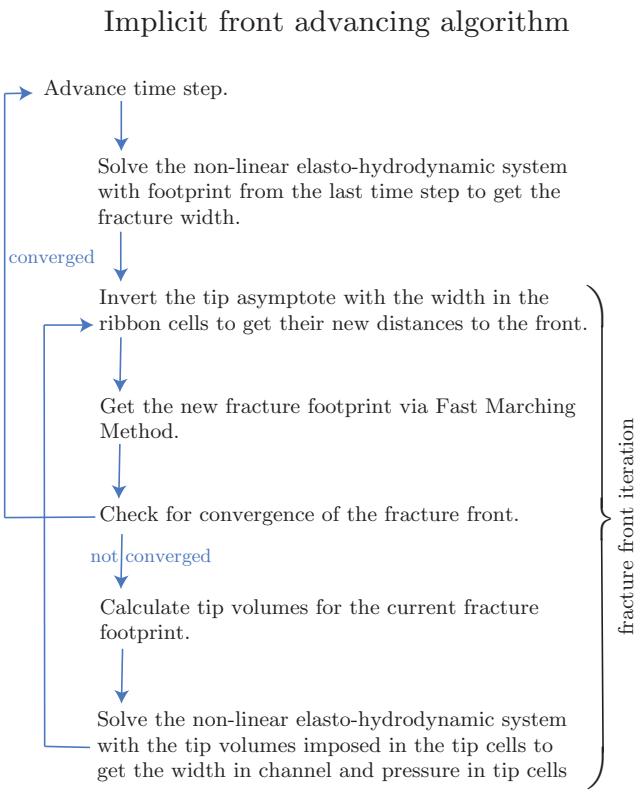

Figure 2: Flow chart of the implicit level set algorithm over a time step.

the non-linear elasto-hydrodynamic system needs to be solved for each iterate of the new fracture front position. An alternative to this scheme is that instead of iterating on the propagation velocity, the change in velocity between successive time steps is assumed to be negligible and the fracture is propagated with the velocity computed at time t^n (at the last time step). The elasto-hydrodynamic system is then solved with the new footprint to get the new width at time t^{n+1}. The velocity at time t^{n+1} (to be used to propagate the front in the next time step) is then obtained by inversion of the tip asymptote using the newly calculated width in the ribbon cells. Such an explicit front advance, of course, introduces error which may cause the fracture front to overshoot or undershoot in the case of decelerating and accelerating front and may lead to oscillations in the solution, making the scheme less robust. We describe below the steps involved in propagating the fracture for a time step with the explicit front advancing algorithm and discuss the implications on the accuracy and stability in later sections.

Propagating with the velocity from the previous time step. To propagate the fracture for the given time step Δt, the signed distance function s^{n+1} for the new time t^{n+1} is initialized in the ribbon cells using the velocity at time t^n:

$$s^{n+1}_{\mathrm{R}^n} = s^n_{\mathrm{R}^n} - V^n_{R^n}\Delta t, \tag{4}$$

where the subscript R^n denotes the ribbon cells from the footprint of the last time step. The distance function is then propagated outward through the rest of the grid with the Fast Marching Method in order to construct the new fracture front position.

Tip volume calculation. The fracture tip volumes are calculated in the same manner as in the implicit scheme although the tip asymptote here is integrated using the velocity from the previous time step.

Solution of the elasto-hydrodynamic system. The elasto-hydrodynamic system is constructed with the new fracture footprint and the tip volumes, and is solved with fixed point iteration to get the fracture width in the channel cells. It is worth pointing out here that such a non-linear system is solved only once over a time-step in such an explicit front advance scheme.

Computation of the new fracture velocity. The newly evaluated width of the ribbon cells is used to invert the tip asymptote to get the distance of the ribbon cells

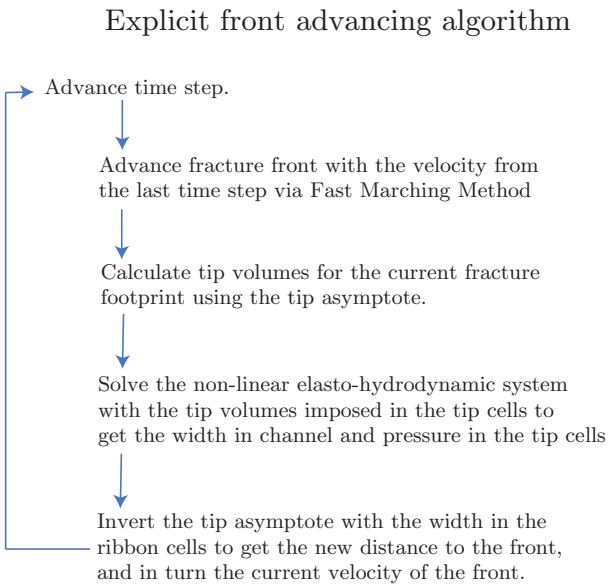

Figure 3: Flow chart describing the steps taken by the explicit front advancing variant of the implicit level set algorithm over a time step.

to the front $s^{n+1}_{\mathrm{R}^{n+1}}$. The velocity of the front is then evaluated by

$$V^{n+1}_{\mathrm{R}^{n+1}} = \frac{s^{n+1}_{\mathrm{R}^{n+1}} - s^{n}_{\mathrm{R}^{n+1}}}{\Delta t}, \tag{5}$$

where the subscript $\mathrm{R}^{\boldsymbol{n+1}}$ denotes the set of ribbon cells from the advanced footprint. These velocities are then used to propagate the fracture front during the next time step. Such an explicit front advancing scheme is summarized in Figure 3.

3.3. predictor corrector front advance

In the implicit front advancing algorithm, the first trial location to start the fracture front iteration is found by a balloon like inflation of the fracture using the footprint of the previous time step. A better guess for the new front location may be obtained by using the available, yet unused, local front velocities from the last time step. These velocities can be used to advance the fracture front to get a first trial position of the front explicitly and the iterations can then be proceeded

in the same manner as the implicit front advancing algorithm until convergence. By starting from this better trial front position, convergence can be attained with potentially less iterations for the same accuracy as compared to the implicit front advancing algorithm. Such a predictor corrector front advancing algorithm is effectively a combination of both the implicit and explicit algorithms. The steps involved are shown in the form of a flow chart in Figure 4.

4. Time stepping strategy

Hydraulic fractures propagate quasi-statically, and under a constant injection rate, their velocity decreases with time. It is therefore computationally efficient to increase the time-step as the fracture grows instead of keeping it constant. More generally, one can adapt the time step such that the increase of the fracture front is roughly equal to one cell size over the next time-step:

$$\Delta t = \lambda \frac{\min(\Delta x, \Delta y)}{\max(V_T)}, \tag{6}$$

where V_T is the front velocities in the tip cells and λ is a prefactor that can be used to control the extent by which the front moves during the next time step. Note that such an adaptive strategy accounts for both the case of accelerating or decelerating fracture.

Although the original implicit algorithm can potentially take large time steps ($\lambda \sim 2$), they cannot be so large that the front jumps over small local heterogeneities without taking them into account. In other words, in order to capture the heterogeneities in the domain up to the resolution of the grid, the front should not move more than the length of one cell over a time step ($\lambda \leq 1$).

In the case of explicit front advancing, the stability of the overall algorithm depends on the front advancing scheme in addition to the convergence of the elasto-hydrodynamics system, which is always ensured for a Backward Euler scheme and a realistic time-step size. The error due to acceleration or deceleration of the front may introduce oscillations in the solution. Note that if the explicit front advancing method is stable and accurate with the prefactor $\lambda = 1$, it would have a major computational advantage over the implicit scheme.

In addition to the above restriction on the time step, we have also added a restriction on the factor by which the fracture can increase its length over a time step. This is necessary in the case of a very coarse mesh at the start of the simulation when the fracture is very small compared to the computational domain. For

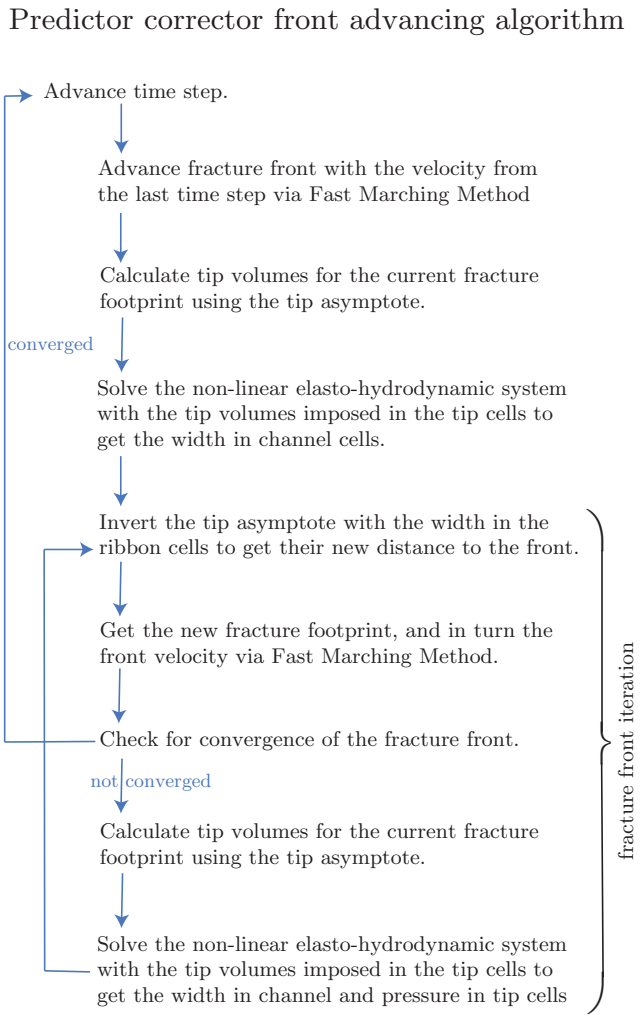

Figure 4: Flow chart describing the steps taken by the predictor corrector front advancing variant of the implicit level set algorithm over a time step.

example, in the extreme case of a radial fracture with initially 5 cells in the fracture along the diameter and having the length of 3 cells (the front being very close to the edge of channel cells in the tip cells), a step size evaluated from Eq. (6) can increase the diameter of the fracture by as much as 2 cell lengths, which is 2/3 of its original length. Such a big change is fracture size may lead to non-convergence of elasto-hydrodynamic solver. We thus evaluate the time step by combining the two restrictions as follows

$$\Delta t = \lambda \min\left(\frac{\min(\Delta x, \Delta y)}{\max(V^T)}, \epsilon \min\left(\frac{\ell^T}{V^T}\right)\right), \tag{7}$$

where $\epsilon \sim 0.08$ is a factor (of the initial length) controlling by which amount the fracture length is restricted to increase over a time step and ℓ^T are the distances of the fracture front from the injection point evaluated in each of the tip cell.

5. Verification and test cases

5.1. Penny shaped hydraulic fracture benchmark

We first test the accuracy of the three front advancing schemes on the case of a penny-shaped hydraulic fracture propagating in a uniform permeable medium due to the injection of a viscous fluid from a point source - see Madyarova [19] for the reference solution. Here, a simulation is performed for a medium having a fracture toughness $K_{Ic} = 0.156$ MPa $\sqrt{\text{m}}$, a plain strain modulus $E' = 3.9 \times 10^{10}$ Pa and a leak-off coefficient $C_L = 0.5 \times 10^{-6}$ m/$\sqrt{\text{s}}$. The fluid driving the fracture growth has a viscosity $\mu = 8.3{\times}10^{-5}$ Pa.s and is injected at a constant rate $Q_o = 0.01$ m^3/s. We divide the square domain of $[-105, 105, -105, 105]$ meters into 81 cells in both the x and y directions.

The simulation is initialized with the viscosity dominated/storage solution (zero leak-off) for a radial hydraulic fracture [20]. It is then propagated under a constant injection rate for a total injection time of 1100 seconds. During the span of the simulation, the fracture propagates in the viscosity/storage propagation regime and move towards viscosity/leak-off regime. The storage to leak-off transition time scale $t_{m\tilde{m}}$ (see e.g. [19, 1] for details of the scalings) corresponding to the simulation parameters is 8.833×10^5 s. Figure 5 shows the radius of the fracture footprint versus time at the top and the fracture efficiency versus time at the bottom respectively, for the three front advancing schemes. For all of the schemes, the solutions are evaluated with three different values of λ (0.6, 0.8 and 1.0) to see if the time step size effects the accuracy of the solution.

It can be seen that all the numerical solutions match the reference solution closely for all the three front advancing schemes and all the different time step prefactors. Note that the solution obtained with the explicit scheme has the same accuracy as the predictor corrector and implicit schemes. The slight error ($< 2\%$) in the fracture efficiency (defined as the ratio of volume of the injected fluid in the fracture to the total injected volume) for all three schemes in the beginning is due to the initialization with the zero leak-off solution. The error in the fracture radius is relatively large ($\sim 4\%$) at the start of the simulation due to course discretization as the number of cells in the fracture are small (~ 4 across the radius). As the fracture grows and more cells enters into the fracture, the error reduces significantly ($\sim 0.5\%$).

To compare the computational efficiency of the different schemes, the number of fracture front iterations taken at each time steps are plotted versus the number of grid elements in the fracture in Figure 6 (top). It can be seen that the predictor corrector scheme, shown in blue, converges more rapidly than the implicit scheme shown in red. In Figure 6 (bottom), we show the CPU time taken by the different front advancing schemes and for different time step prefactors versus the time for which the solution is evaluated. For relative comparison, we scale the CPU times with the maximum CPU time taken by a time step during the implicit scheme. For a Python implementation of the algorithm running on a computer with Intel(R) Core(TM) i7-5600U CPU @ 2.6GHz microprocessor, this largest time step (which corresponds to the largest number of elements) takes 435 seconds. In direct reflection of the number of fracture front iterations, the CPU time is 7 to 8 times, and 4 to 5 time larger for the implicit and predictor corrector schemes respectively as compared to the explicit scheme. Note that the plot is in log-log scale, signifying that the time taken to solve a time step is about two orders of magnitude smaller in the beginning of the simulation when there is a small number of cells in the fracture. As the fracture grows and more cells enters into the fracture, the computational requirement increases from $O(n^2)$ to $O(n^3)$: initially the cost of making the non-linear elasto-hydrodynamics system takes more time than solving it while for larger system size (at larger time), this reverses. This is of course the case here as we use a simple direct solver for the tangent linear system - better performance than $O(n^3)$ can be achieved with more refined approaches to the solution of the elasto-hydrodynamics system [21, 22].

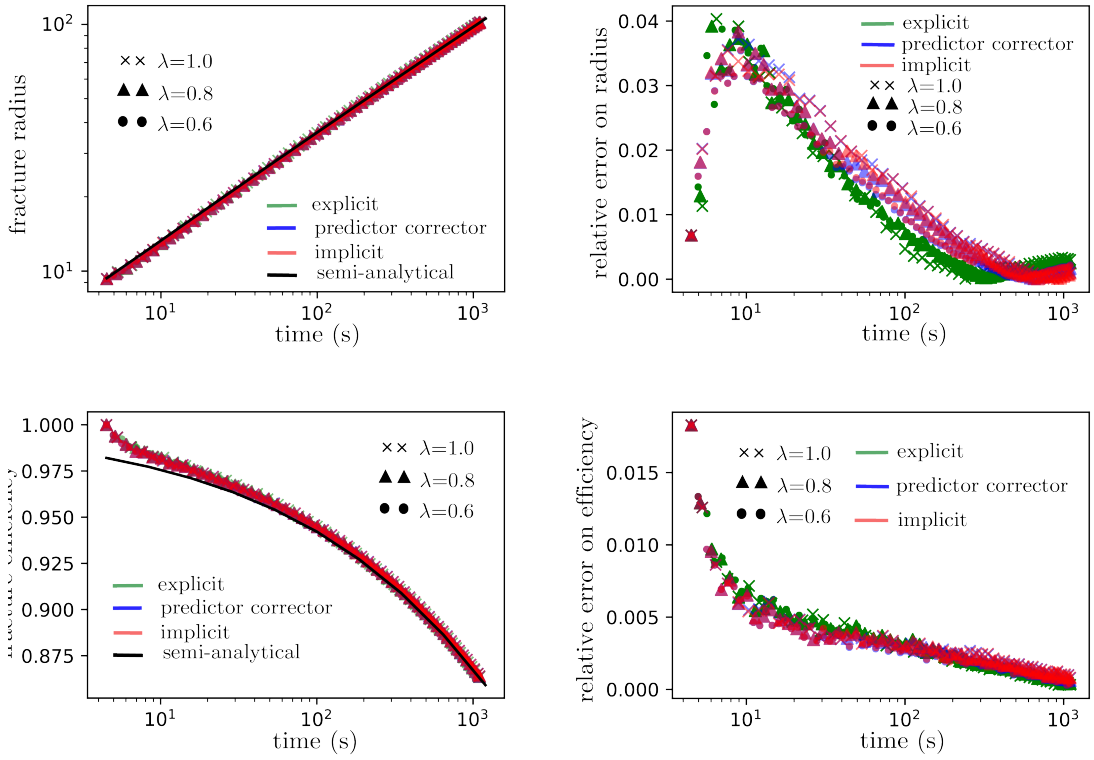

Figure 5: The fracture radius (top) and fracture efficiency (bottom) versus time for a penny shaped hydraulic fracture as evaluated by the explicit, predictor corrector and implicit front advancing schemes. The relative errors with the semi-analytical solution are plotted on the right. Solutions obtained with three different time step prefactors (λ) are shown for each of the front advancing scheme to investigate the impact of time step size on the accuracy of the solution.

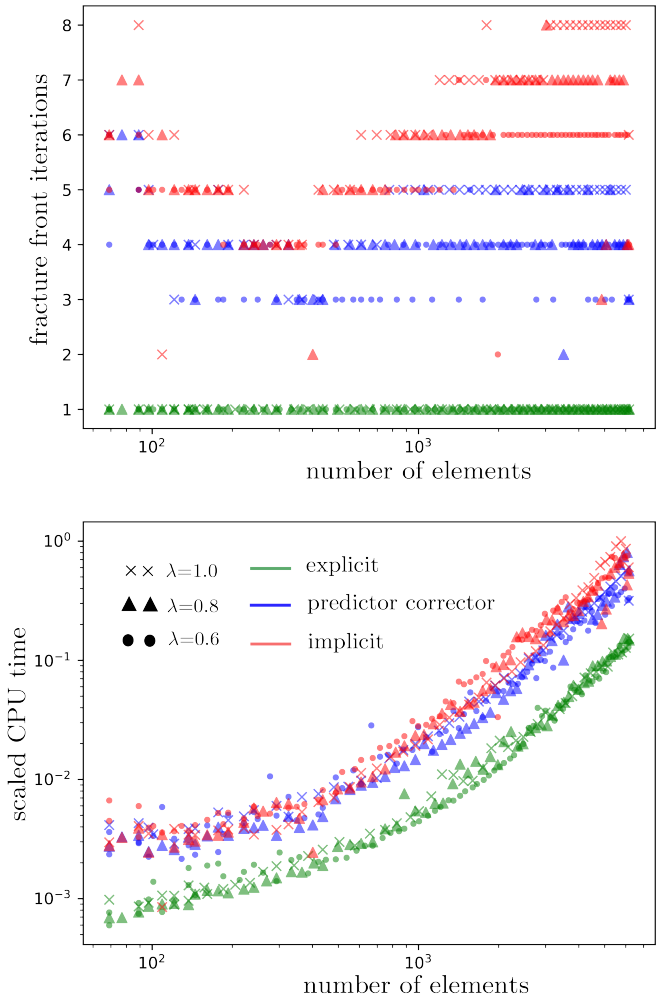

Figure 6: The number of fracture front iterations (top) and scaled CPU time (bottom) as function of the number of elements within the fracture. Penny shaped fracture benchmark for the explicit, predictor corrector and implicit front advancing schemes. Results for three different time step prefactors are shown for each of the front advancing scheme. The symbols used are same in the top and bottom plots.

5.2. Accelerating / decelerating fracture front example

In order to better understand the robustness of the explicit front advancing version of the scheme, we investigate its performance in a case where the fracture front crosses a heterogeneity that will either make the fracture accelerate or decelerate locally. The change in the local fracture front velocity can be caused by a change in material properties of the rock – such as fracture toughness or permeability – or by a variation of the in-situ confining stress. In this test case, we investigate both the acceleration and deceleration of the fracture front by allowing the fracture to enter a layer having a lower confining stress (acceleration case) or a larger confining stress (deceleration case) as depicted in figure 7.

In the first part of the test case, we consider a fracture that is propagating in a uniform impermeable medium, driven by a fluid with a viscosity of 1 Pa.s injected at a constant rate of 1×10^{-4} m^3/s. The fracture toughness is assumed to be negligible, i.e. the fracture propagates in the so-called viscosity dominated regime. To investigate the effect of acceleration of the fracture front, a layer with much lower confining stress (2 MPa as compared to 30 Mpa in the layer where the fracture is initiated) is set up on top (see Figure 7, top). Under these conditions, the fracture is expected to propagate as a radial fracture initially, and then accelerate along the vertical direction (y-axis) as it enters the upper layer. The configuration is simulated with the three different front advancing schemes to investigate their performance. As the performance of the explicit front advancing scheme is dependent on the time step, the results are first compared for simulations performed with three different constant time steps of 6ms, 8ms and 10ms for all three schemes. These time steps are equivalent to taking $\lambda = 1.05$, 1.40 and 1.75 respectively together with the velocity of the fracture front just after entering the upper layer. Results are also compared using adaptive time stepping with different prefactors λ of 0.6, 0.8 and 1.0.

Figure 8, shows the time evolution of the distance of the front from the injection point along the y-axis (represented as ℓ in Figure 7) as evaluated with the predictor corrector and explicit schemes. For comparison, the distances are normalized with the corresponding distances evaluated with the implicit scheme. It can be seen that the predictor corrector scheme gives virtually the same solution as the implicit scheme (the relative difference is of the order $\sim 10^{-3}$). The explicit solution also closely follows the implicit solution until the front enters the upper layer and undershoots the front position as the front is propagated with lower velocity of the last time step. This causes the solution to oscillate in the next few time steps, until it recovers and converges to the correct solution as the fracture propagates further into the upper layer. Figure 9 shows the time evolution of the

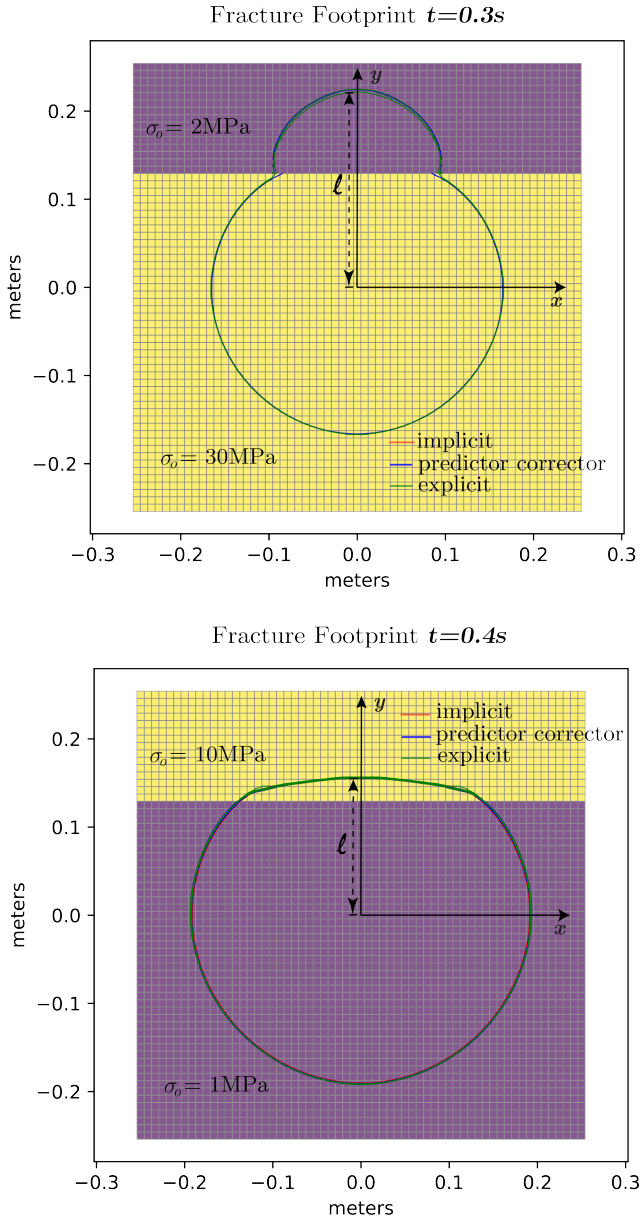

Figure 7: Fracture footprint as evaluated by the explicit (shown in green), predictor corrector (shown in blue) and implicit (shown in red) front advancing schemes. There are three plots for each of the front advancing scheme corresponding to three different time step prefactors (λ = 0.6, 0.8, 1.0). The top and bottom figures show the cases of an accelerating and decelerating fracture front respectively.

normalized distance ℓ/ℓ_{imp} given by the two scheme for the same setup, but evaluated with adaptive time stepping with prefactors λ of 0.6, 0.8 and 1.0. Similar results, compared to the fixed time stepping, are observed except the oscillations are significantly subdued due to relatively smaller time steps taken as the velocity of the front increases upon entering the upper layer. Figure 7 (top) shows that the footprint is virtually indistinguishable for all the solutions at the final time of 0.3 s.

In a second test, a layer with a confining stress of 10 Mpa is set up on top of a layer with a confining stress of 1 MPa to investigate the case of deceleration of the front (see Figure 7). The rest of the parameters are similar to the acceleration test case previously discussed. The explicit scheme expectedly overshoots the front position as it enters the upper layer. Figure 10 shows the normalized distance ℓ/ℓ_{imp} evaluated by the implicit and explicit scheme respectively, for the three different fixed time steps of 12ms, 16ms and 20ms. These time steps are equivalent of $\lambda = 0.46$, 0.61 and 0.77 respectively, calculated with the velocity of the front just after entering the upper layer. Results from the adaptive time stepping with prefactors of 0.6, 0.8 and 1.0 are also shown in Figure 11. The results are similar to the previous accelerating case, with the expected difference of an overshooting of the front position instead of an undershooting by the explicit front advancing scheme. Figure 7 shows that the footprint is virtually indistinguishable for all the schemes.

5.3. Comparison with a laboratory experiment

Finally, we numerically replicate a viscosity dominated laboratory experiment [23] in which a hydraulic fracture grows into a layer with lower confining stress while being bounded by another layer of larger confining stress. This provides a good test for the validity of the mathematical model as well as for the performance of the overall numerical algorithm, including the three different front advancing schemes. The experiment consists of injection of a fluid with a viscosity of 30 Pa.s into a PMMA block in a three layers configuration (see the above referenced paper for details). Different confining stresses are applied in three layers with the upper layer having a larger confining stress layer of 11 MPa, the lower layer having a confining stress of 5 MPa and the layer in the middle (of 50 mm height) that contains the injection point having a confining stress of 7 MPa (see Figure 12). The others parameters are as follows

$$E' = 3.9 \times 10^{10} \text{ Pa},\ K_{Ic} = 0,\ C_L = 0,\ \mu = 30 \text{ Pa.s},\ Q_o = 0.0023 \text{ mL/s}.$$

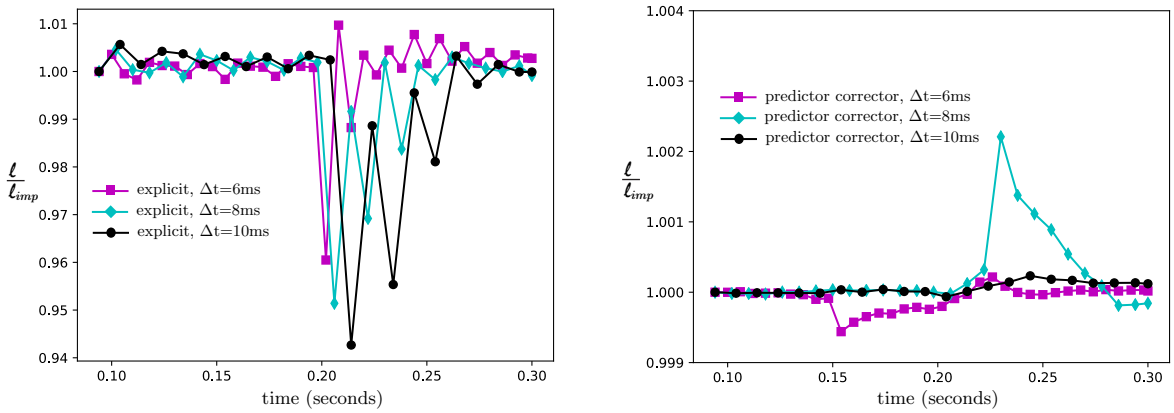

Figure 8: Normalized distance of the front along the y-axis from the injection point for the fracture front acceleration test case. The left and right figures show the solution evaluated by the explicit and predictor corrector front advancing schemes respectively using three different time step sizes of 6ms, 8ms and 10ms.

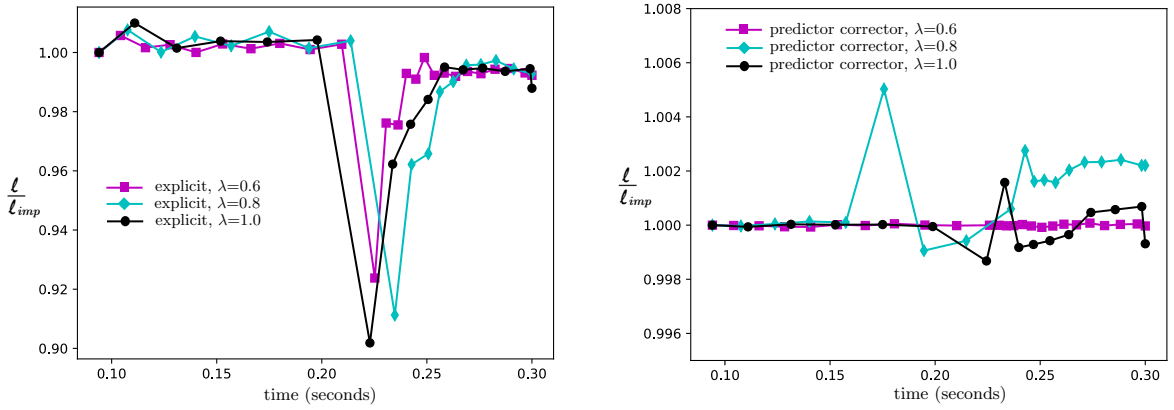

Figure 9: Normalized distance of the front along the y-axis from the injection point for the fracture front acceleration test case. The left and right figures show the solution evaluated by the explicit and predictor corrector front advancing schemes respectively using three different time step prefactors (λ) of 0.6, 0.8 and 1.0.

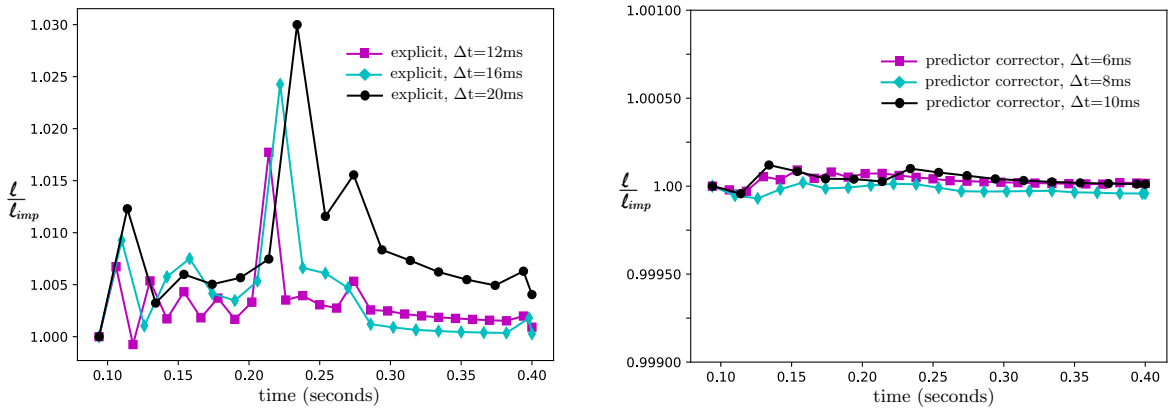

Figure 10: Normalized distance of the front along the y-axis from the injection point for the fracture front deceleration test case. The left and right figures show the solution evaluated by the explicit and predictor corrector front advancing schemes respectively using three different time step sizes of 12ms, 16ms and 20ms.

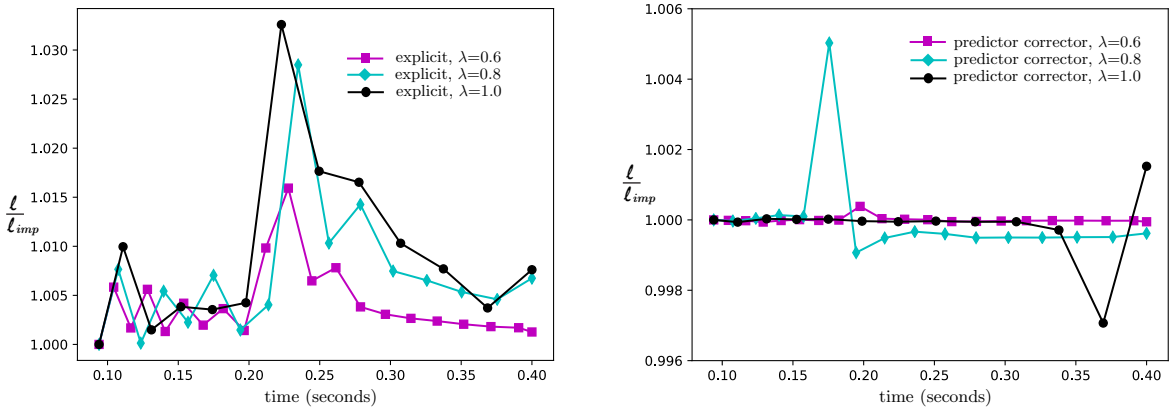

Figure 11: Normalized distance of the front along the y-axis from the injection point for the fracture front deceleration test case. The left and right figures show the solution evaluated by the explicit and predictor corrector front advancing schemes respectively using three different time step prefactors (λ) of 0.6, 0.8 and 1.0.

	Fracture Front Iterations	CPU Time	CPU Time Ratio
Implicit	257	619 s	4.04
predictor corrector	210	492 s	3.21
Explicit	48	153 s	1.00

Table 1: The performance comparison of the three front advancing schemes for the numerical simulation of the laboratory experiment. First column shows the total number of fracture front iterations (equivalently, the number of times the non-linear elasto-hydrodynamic system is solved) taken by the three schemes to simulate the total time of 665 s. Second column shows the CPU time taken by the three schemes (on a Intel(R) Core(TM) i7-5600 CPU - 2.6GHz). The time taken by the implicit and the predictor corrector schemes relative to the explicit scheme are shown in the third column.

Due to a rather large injection line, the effective injection rate entering the fracture varies with time due to fluid compressibility effects during the initial pressurization phase (see [24] for discussion). The evolution of the injection rate into the fracture can be approximated here by three constant injection steps: 0.0009 mL/s for the first 31 seconds, 0.0065 mL/s for the next 120 seconds and 0.0023 mL/s for the rest of the experiment.

We perform simulation of this laboratory experiment with the level set algorithm previously described, using the three different front advancing schemes. The rectangular domain of [-0.13, 0.13, -0.17, 0.17] meters was divided into 61 cells in the x direction and 79 cells in the y direction. A λ of 1.0 was used to evaluate the adaptive time step. Figure 12 displays the fracture footprint at $t = 22$ s, 60 s, 144 s, 376 s and 665 s for the different front advancing schemes as well as the experimental measurements. Very good agreement between the experimental and numerical results computed with all three schemes can be seen. Table 1 summarizes the total number of fracture front iterations (signifying the number of times the non-linear elasto-hydrodynamic system is solved) performed by the three front advancing schemes to compute the solution up to 665 seconds. The CPU time shown are for a Python implementation of the algorithm running on an Intel(R) Core(TM) i7-5600 CPU - 2.6GHz microprocessor. It can be seen that the predictor corrector and the implicit schemes are respectively about 3 and 4 times more costly than the explicit front advancing scheme.

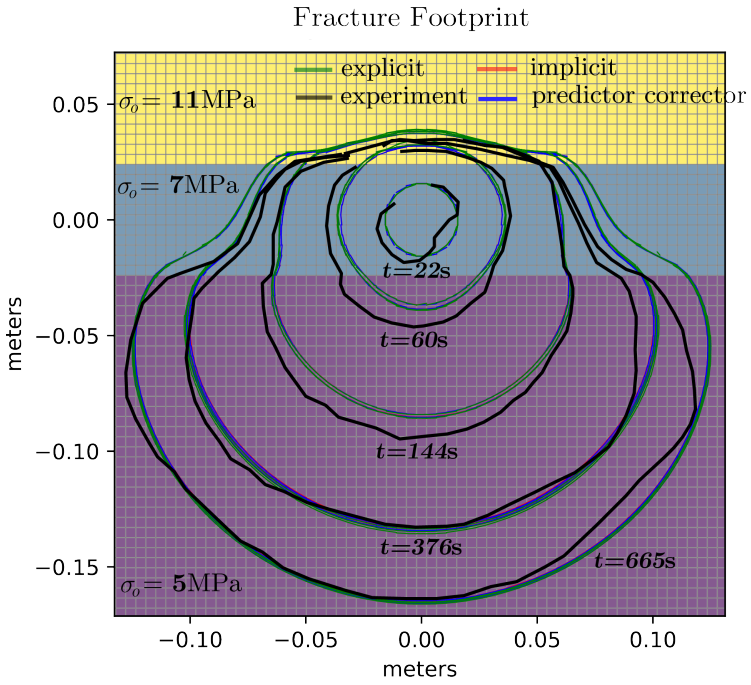

Figure 12: Fracture footprint as evaluated by the explicit (shown in green), predictor corrector (shown in blue) and implicit (shown in red) front advancing schemes for the three layers hydraulic fracture experiment of [23]. The experimental results are shown in black.

6. Conclusions

One of the major challenge for the simulation of hydraulic fracture growth lies in the proper resolution of the evolving fracture front. The Implicit level set algorithm (ILSA) originally developed in [8] uses the level set method in conjunction with the hydraulic fracture tip asymptotic solution [7] to provide a highly accurate and efficient algorithm to locate the moving boundary. ILSA advances the fracture front via a fully implicit scheme: i.e. the final location of the front is found by iterating on the front position until it converges. This implicit scheme, although robust and accurate, is computationally costly due to the iterations required to obtain the new fracture front position. In this paper, we have investigated a variant of this scheme where the fracture front is advanced either entirely explicitly, using the velocity of the previous time step or in a predictor corrector manner, using the explicit step as first guess for the implicit scheme. It is important to bear in mind that although the fracture front advance is performed explicitly, the elasto-hydrodynamics system is solved with an implicit/backward Euler scheme in order to circumvent the stringent CFL condition of such system [2].

We have tested the stability of the explicit scheme for a challenging test case where the fracture front accelerate after moving into a layer with a confining stress 15 times less than the layer from which it enters. An extreme test configuration unlikely to happen in practice. We have shown that the explicit version of the scheme introduces a slight error in the solution (few percents) in the case of an accelerating or decelerating fracture front, which may cause the solution to oscillate sporadically over few time-steps. The oscillations are however damped quickly if the time step is dynamically adapted as a function of the velocity of the fracture front.

For all the test cases, we observe that the solution obtained with the explicit front advancing scheme matches closely to the solution of the implicit scheme but is around ~ 4 times faster computationally. The difference between the solutions evaluated by the two schemes is of a few percents in the few time steps after the fracture front hits a heterogeneity. It is important to note that such an error might accumulate in the case where multiple heterogeneities are present at the scale of a few grid cells. In such a very heterogeneous configuration, either a finer mesh or a smaller time step (or a combination of the two) is to be used in conjunction with the explicit front advancing scheme. In any case, the predictor corrector scheme always performs similarly to the implicit scheme both in terms of accuracy and stability but requires 25% to as much as 50% percent less computational time. It is therefore the preferred scheme to be used in all cases, while the explicit scheme is

favored in relatively homogeneous configurations or when a first "quick" solution is sought for.

Acknowledgements

This work was funded by the Swiss National Science Foundation under grant #160577.

References

[1] E. Detournay, Mechanics of hydraulic fractures, Annual Review of Fluid Mechanics 48 (2016) 311–339.

[2] J. Adachi, E. Siebrits, A. Peirce, J. Desroches, Computer simulation of hydraulic fractures, International Journal of Rock Mechanics and Mining Sciences 44 (2007) 739–757.

[3] B. Lecampion, A. P. Bunger, X. Zhang, Numerical methods for hydraulic fracture propagation: A review of recent trends, Journal of Natural Gas Science and Engineering 49 (2018) 66–83.

[4] D. Garagash, E. Detournay, The tip region of a fluid-driven fracture in an elastic medium, Transactions-American Society of Mechanical Engineers Journal of Applied Mechanics 67 (2000) 183–192.

[5] D. I. Garagash, E. Detournay, Plane-strain propagation of a fluid-driven fracture: Small toughness solution, Journal of Applied Mechanics 72 (2005) 916.

[6] D. I. Garagash, Scaling of physical processes in fluid-driven fracture: perspective from the tip, in: F. Borodich (Ed.), IUTAM Symposium on Scaling in Solid Mechanics, volume 10 of *IUTAM Bookseries*, Springer, Dordrecht, 2009, pp. 91–100.

[7] D. I. Garagash, E. Detournay, J. I. Adachi, Multiscale tip asymptotics in hydraulic fracture with leak-off, Journal of Fluid Mechanics 669 (2011) 260–297.

[8] A. Peirce, E. Detournay, An implicit level set method for modeling hydraulically driven fractures, Computer Methods in Applied Mechanics and Engineering 197 (2008) 2858–2885.

[9] J. Desroches, E. Detournay, B. Lenoach, P. Papanastasiou, J. Pearson, M. Thiercelin, A. Cheng, The crack tip region in hydraulic fracturing, in: Proceedings of the Royal Society of London A: Mathematical, Physical and Engineering Sciences, volume 447, The Royal Society, pp. 39–48.

[10] B. Lenoach, The crack tip solution for hydraulic fracturing in a permeable solid, Journal of the Mechanics and Physics of Solids 43 (1995) 1025–1043.

[11] B. Lecampion, A. Peirce, E. Detournay, X. Zhang, Z. Chen, A. Bunger, C. Detournay, J. Napier, S. Abbas, D. Garagash, et al., The impact of the near-tip logic on the accuracy and convergence rate of hydraulic fracture simulators compared to reference solutions, in: Effective and sustainable hydraulic fracturing, InTech, 2013.

[12] A. Peirce, Modeling multi-scale processes in hydraulic fracture propagation using the implicit level set algorithm, Computer Methods in Applied Mechanics and Engineering 283 (2015) 881–908.

[13] A. Peirce, Implicit level set algorithms for modelling hydraulic fracture propagation, Philosophical Transactions of the Royal Society A: Mathematical, Physical and Engineering Sciences 374 (2016) 20150423.

[14] E. Detournay, A. Peirce, On the moving boundary conditions for a hydraulic fracture, International Journal of Engineering Science 84 (2014) 147–155.

[15] E. Dontsov, A. Peirce, A multiscale implicit level set algorithm (ilsa) to model hydraulic fracture propagation incorporating combined viscous, toughness, and leak-off asymptotics, Computer Methods in Applied Mechanics and Engineering 313 (2017) 53–84.

[16] S. L. Crouch, A. M. Starfield, F. Rizzo, Boundary element methods in solid mechanics, Journal of Applied Mechanics 50 (1983) 704.

[17] B. Lecampion, E. Detournay, An implicit algorithm for the propagation of a hydraulic fracture with a fluid lag, Computer Methods in Applied Mechanics and Engineering 196 (2007) 4863–4880.

[18] D. I. Garagash, Propagation of a plane-strain fluid-driven fracture with a fluid lag: early-time solution, International Journal of Solids and Structures 43 (2006) 5811–5835.

[19] M. V. Madyarova, Fluid-driven penny-shaped fracture in elastic medium, Ph.D. thesis, University of Minnesota, 2003.

[20] A. Savitski, E. Detournay, Propagation of a penny-shaped fluid-driven fracture in an impermeable rock: asymptotic solutions, International Journal of Solids and Structures 39 (2002) 6311–6337.

[21] A. P. Peirce, Localized jacobian ILU preconditioners for hydraulic fractures, International Journal for Numerical Methods in Engineering 65 (2006) 1935–1946.

[22] A. Peirce, E. Siebrits, A dual mesh multigrid preconditioner for the efficient solution of hydraulically driven fracture problems, International journal for numerical methods in engineering 63 (2005) 1797–1823.

[23] R. Wu, A. Bunger, R. Jeffrey, E. Siebrits, et al., A comparison of numerical and experimental results of hydraulic fracture growth into a zone of lower confining stress, in: The 42nd US Rock Mechanics Symposium (USRMS), American Rock Mechanics Association.

[24] B. Lecampion, J. Desroches, R. G. Jeffrey, A. P. Bunger, Experiments versus theory for the initiation and propagation of radial hydraulic fractures in low permeability materials, Journal of Geophysical Research: Solid Earth 122 (2017).